

In-situ Monitoring of Temperature, Flow and Pressure in Micro Methanol Reformer by Embedded Integrated Multifunction Micro Sensor

Chi-Yuan Lee^{*}, Chia-Chieh Shen, Fan-Hsuan Liu, Yu-Ming Chang

Department of Mechanical Engineering, Yuan Ze Fuel Cell Center, Yuan Ze University, Taoyuan, Taiwan

*E-mail: cylee@saturn.yzu.edu.tw

Received: 2 March 2013 / Accepted: 19 March 2013 / Published: 1 April 2013

Methanol can be used as the hydrogen source for the operation of fuel cells, given its features of safe storage and transportation management, as well as low reforming temperature (250~300°C). The micro reformer can convert methanol into hydrogen for portable fuel cells, resulting in many advantages. This study integrated micro temperature, flow and pressure sensors using the micro-electro-mechanical systems (MEMS) technology, and embedded integrated multifunction micro sensor in the micro reformer, so as to measure the distributions of temperature, flow and pressure simultaneously for real-time diagnosis. This study also discussed the internal reaction mechanism of micro reformer, and identified the internal reaction of micro reformer correctly for real-time monitoring and adjustment. This study was consisted of two parts: 1) integration of micro sensor: the polyimide (PI) film is used as substrate to develop the micro temperature, flow and pressure sensors; 2) real-time monitoring of micro reformer: the integrated multifunction micro sensor is embedded in the micro reformer for real-time microscopic monitoring of the changes in temperature, flow and pressure.

Keywords: Micro reformer, integration micro sensor, real-time microscopic monitoring

1. INTRODUCTION

Considering limited natural resources and depletion of various fossil energy sources, many countries around the world are developing new green energy. Fuel cell has attracted special attention among different kinds of green energy for its high generating efficiency, extensive application and easy fuel acquisition. Its technology has matured gradually.

The fuels for fuel cells are oxygen and hydrogen, and the methanol reformer is extensively used for obtaining hydrogen. The hydrogen generated by the reformer can be supplied to the proton exchange membrane fuel cell.

Pan [1] designed a methanol reformer that could be started up at room temperature, and studied different operating parameters in methanol reforming reaction. The results showed that the optimal methanol and air flow rates were 0.55 ml/min and 3 l/min respectively. The methanol reforming reaction could provide high concentration hydrogen (above 73%) and the system efficiency was kept above 74%, suggesting a good stability.

Chein [2] used quartz tubes to make a small sized reformer with a diameter of 17mm and a length of 60mm. The experimental results showed that the maximum methanol conversion was 97%, the minimum CO concentration was 90 ppm, and the maximum power density was 0.8 kW/L.

D' Aleo [3] made an array of temperature sensors on glass substrate, and used platinum as the sensing head and gold as conductor. Aluminium oxide was deposited as protective layer. The temperature measurement range was 0~200°C.

Shikida [4] used photolithography process to make a flow sensor on 25µm polyimide film (PI film), and monitored the flow rate at the outlet of the air-conditioning system of a building to reduce meaningless energy waste.

This study developed a single micro temperature sensor for the actual temperature distribution in the micro methanol reformer in the past [5, 6], and used the flexible high molecular material, PI as the substrate, and integrated the temperature, flow and pressure sensors into an integrated micro pressure, temperature and flow sensor. This study further improved the dielectric layer material in the capacitive micro pressure sensor of the integrated multifunction micro sensor, and embedded the integrated multifunction micro sensor in the micro reformer to measure the distribution of temperature, flow and pressure in the micro reformer during reaction and to record the measured data instantly. The data were analyzed for studying the improvement of reformer operating parameters and structure design in order to obtain the optimal methanol conversion efficiency.

2. METHODOLOGY

2.1. Micro Temperature Sensor

This study used the resistance temperature detector (RTD). The electrical resistance increased with the temperature rise detected by the detector, and the increase amplitude depended on the positive temperature coefficient (PTC) α .

The change in the resistance value of temperature sensitive resistor can be defined as Eq. (1):

$$R_t = R_0(1 + \alpha\Delta T + \beta\Delta T^2) \quad (1)$$

where α and β are constants, as the measured temperature difference is small, Eq. (1) can be reduced to:

$$R_t = R_0(1 + \alpha\Delta T) \quad (2)$$

$$\Delta T = t - t_0 \quad (3)$$

where R_t is the electrical resistance of the temperature at $t^\circ\text{C}$; R_0 is the electrical resistance of temperature at 0°C ; α is the resistance temperature coefficient of temperature sensitive resistor material; ΔT is the temperature difference to the reference temperature; t is the temperature at $t^\circ\text{C}$; t_0 is the reference temperature of the resistor [7].

The electrode of the micro temperature sensor used in this study was designed as serpentine structure. The temperature sensing area is $620\mu\text{m} \times 600\mu\text{m}$, as shown in figure 1.

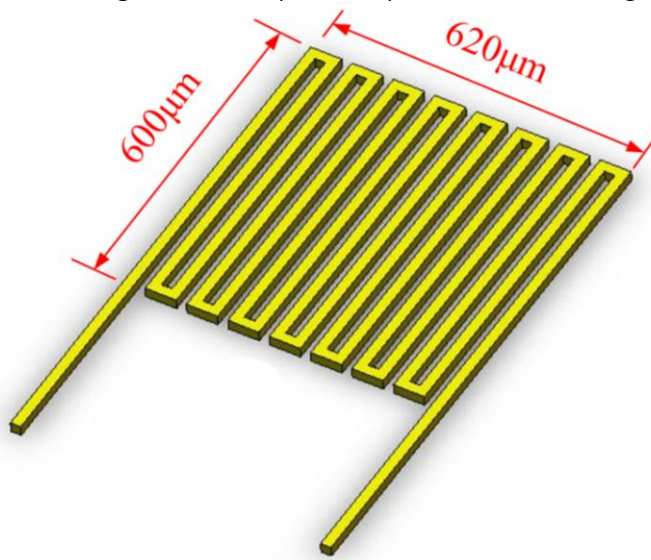


Figure 1. The design of the micro temperature sensor.

2.2. Micro Flow Sensor

This study used hot-wire flow sensor, composed of a heater, as shown in figure 2. The heater was placed in a flow field and applied with fixed voltage to form a stable temperature field. The fluid carried heat away when it flew through the heater, so as to change the electrical resistance of the heater. According to Ohm's law, when the voltage is fixed, the current increases as the resistance decreases, so that the relation curve of current and flow rate can be obtained to obtain the flow rate of flow field.

According to King's deduction of hot-wire flow sensor, the relation between the heat dissipation rate of hot wire and the fluid flow rate is shown as Eq. (4).

$$Q = I^2 \times R = I \times V = (A + B \times U^n) (T_s - T_o) \quad (4)$$

where Q is the power supplied from external power supply to the hot wire; U is the flow rate of fluid; T_s is the temperature of hot wire; T_o is the temperature of fluid; n is the correlation coefficient of U and Q ; A is a constant, when the flow rate is fixed at zero, the coefficient of heat transferred by the heater; B is also a constant, when the flow rate is not zero, the coefficient of heat transferred by the fluid and heater. Eq. (4) can be changed to Eq. (5) [8].

$$Q = (A + B \times U^{0.5}) \Delta T \quad (5)$$

The electrode of the micro flow sensor used in this study was designed as serpentine structure, and the flow rate sensing area was $940\mu\text{m} \times 600\mu\text{m}$, as shown in figure 3.

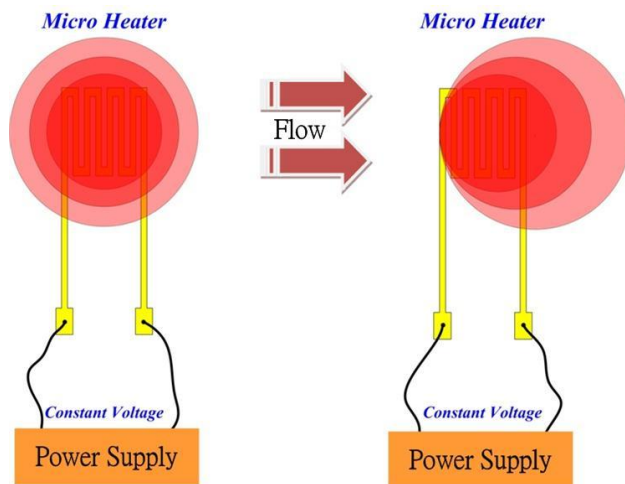


Figure 2. The methodology of the hot-wire flow sensor.

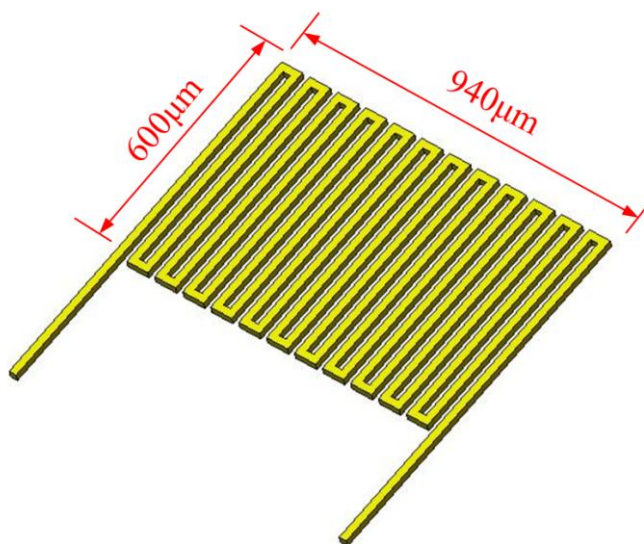


Figure 3. The design of the micro flow sensor.

2.3. Micro Pressure Sensor

The dielectric layer of the capacitive pressure sensor used in this study was changed from PDMS (polydimethylsiloxane) material to high molecular material PI 7320. The two materials were compared in table 1. The PI 7320 was easier to define the location of dielectric layer than PDMS, and the dielectric constant was better.

The capacitive pressure sensor is unlikely to be influenced by temperature, and it is very sensitive, thus, it is applicable to the environment with large temperature change and small pressure change in the micro reformer. The general capacitive pressure sensor is shown in figure 4, composed of two parallel electrodes. The dielectric layer is between them, and the computing formula for the capacitance value of sensor is Eq. (6).

$$C = \epsilon_r \epsilon_0 \frac{A}{d} \tag{6}$$

where ϵ_r is the dielectric constant of material; ϵ_0 is the fixed value 8.854×10^{-12} (F/m); A is the overlap area of upper and lower electrodes; d is the distance between two parallel electrodes. Therefore, the d value changes when the pressure sensor is compressed, and the variance in the capacitance value is measured, so as to obtain the variation in the pressure value [9]. The sensing area of the micro pressure sensor used in this study is $1200\mu\text{m} \times 800\mu\text{m}$.

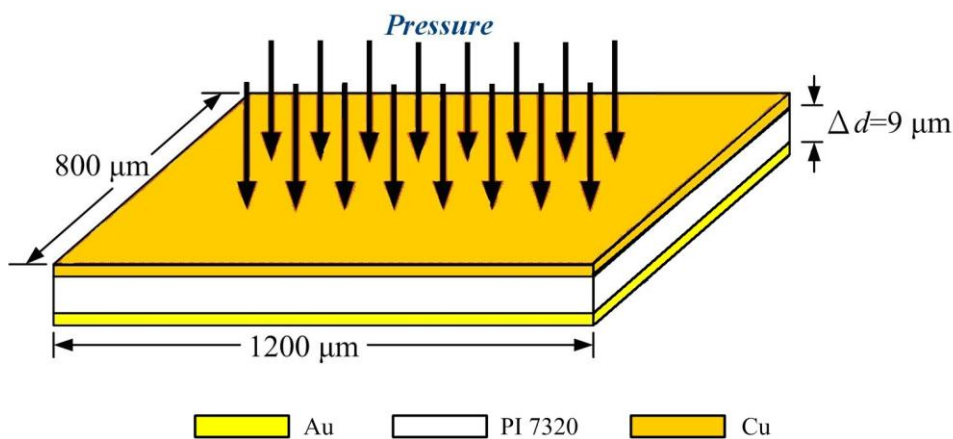


Figure 4. The methodology of the capacitive pressure sensor.

Table 1. The comparison of material properties.

	PDMS	PI 7320
Young's Modulus	750kPa	2.5GPa
Dielectric constant	2.65	3.2

3. FABRICATION

The substrate of the integrated multifunction micro sensor used in this study was PI film. The production process is shown in figure 5.

First, the substrate was soaked in acetone solution and oscillated in ultrasonic oscillator for 5 min, and then operated in methanol solution. Its surface was cleaned with DI water, and oven dried. The E-beam evaporator was used to evaporate adhesion layer chrome (Cr, 400Å) and electrode layer gold (Au, 2000Å) on the substrate by vaporization. The spin coater coated photoresist (AZP4620) on one side of substrate, and the aligner and mask were used for pattern transfer for the photoresist. MP2500 and H₂O were mixed in the ratio of 1:5 to make developer to develop the required pattern. The gold and chrome were etched, and then the photoresist was removed, so as to finish the bottom electrodes of micro temperature and micro flow sensors (figure 6) and micro pressure sensor.

The PI 7320 was spin coated on one side of the substrate of defined pattern. The capacitor dielectric layer of micro pressure sensor was defined by photolithography process, and the E-beam

evaporator was used to coat 2000Å copper (Cu) by vaporization. The upper electrode layer of micro pressure sensor was completed by lithography and etching processes. The completed micro pressure sensor is shown in figure 7.

PI 7505 was spin coated on the substrate as the upper insulating layer, and the pad was exposed by photolithography process to complete the integrated multifunction micro sensor, as shown in figure 8.

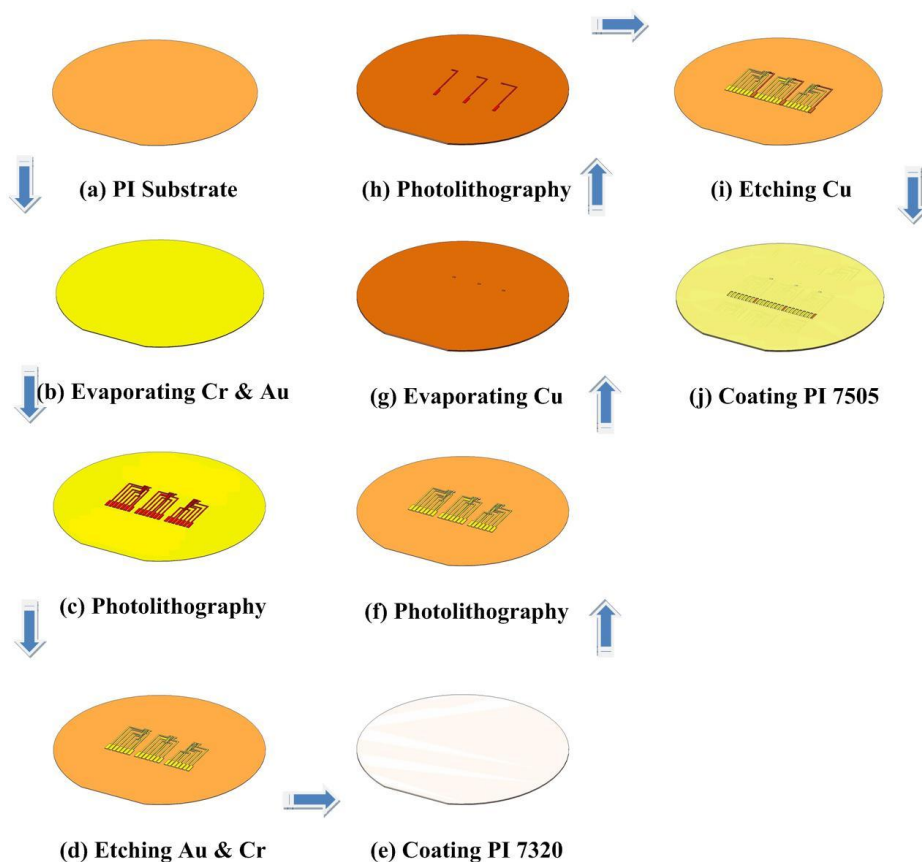


Figure 5. The fabrication of the integrated multifunction micro sensor.

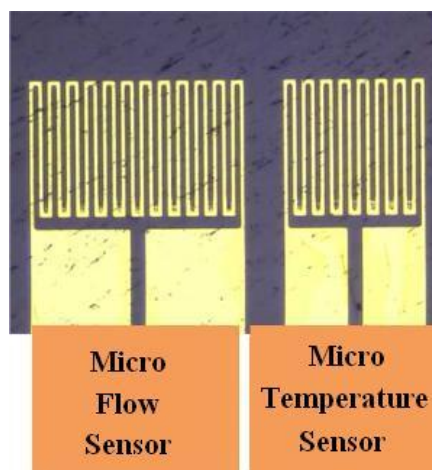


Figure 6. The micro flow and temperature sensors.

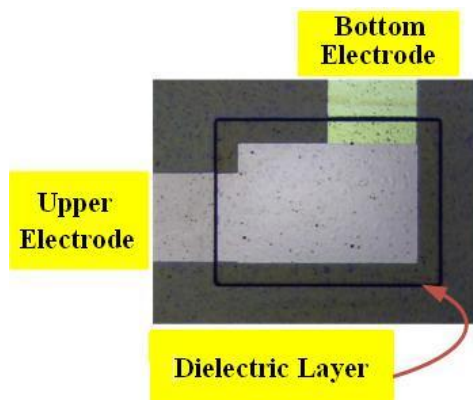


Figure 7. The micro pressure sensor.

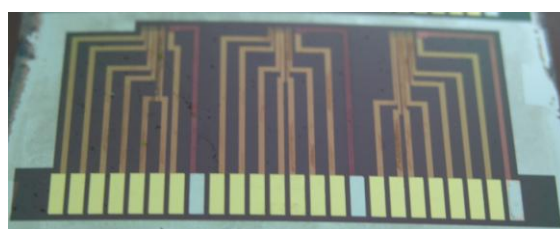


Figure 8. The integrated multifunction micro sensors.

4. RESULTS AND DISCUSSION

4.1. Calibration of Micro Temperature Sensors

The integrated multifunction micro sensor was embedded in the micro reformer, wound with heating tapes and covered with heat retaining cotton, so that the micro reformer could be heated uniformly.

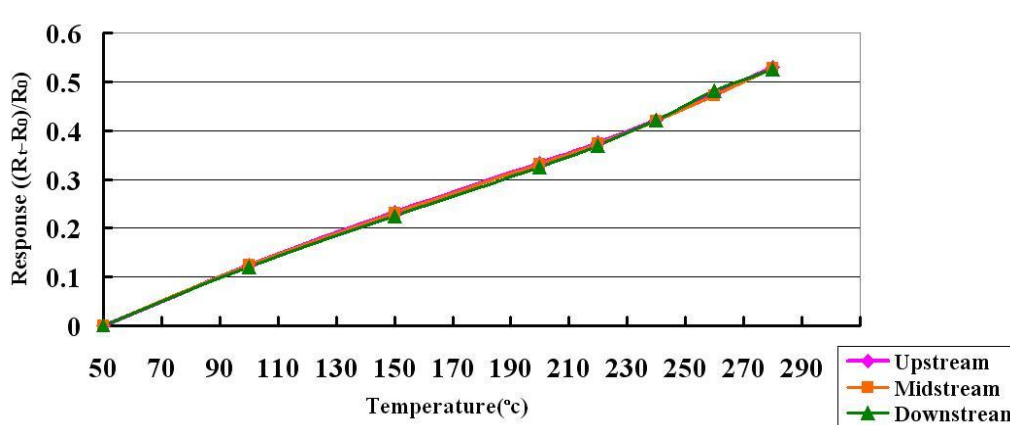


Figure 9. Calibration curves of micro temperature sensor.

This study used NI SCXI 1000 to measure the change in the electrical resistance of micro temperature sensor and recorded the heating temperature values. The obtained temperature correction curve is shown in figure 9.

4.2. Calibration of Micro Flow Sensors

The integrated multifunction micro sensor was located in the upstream, midstream and downstream of flow channel of micro reformer. The reformer was wound with heating tapes and heated to 270°C. The sensor was connected to HOLA DM2750T digital multimeter to measure the current change. When the micro reformer was heated to 270°C, 4V constant voltage was supplied to the flow sensor to make stable temperature field. The fluid was fed for correction.

The flow rate correcting range was 5~50sccm, measured once at intervals of 10sccm. The obtained micro flow sensor correction curve is shown in figure 10, where I_f is the current value measured at flow rate f , I_0 is the current value of the flow rate reference point.

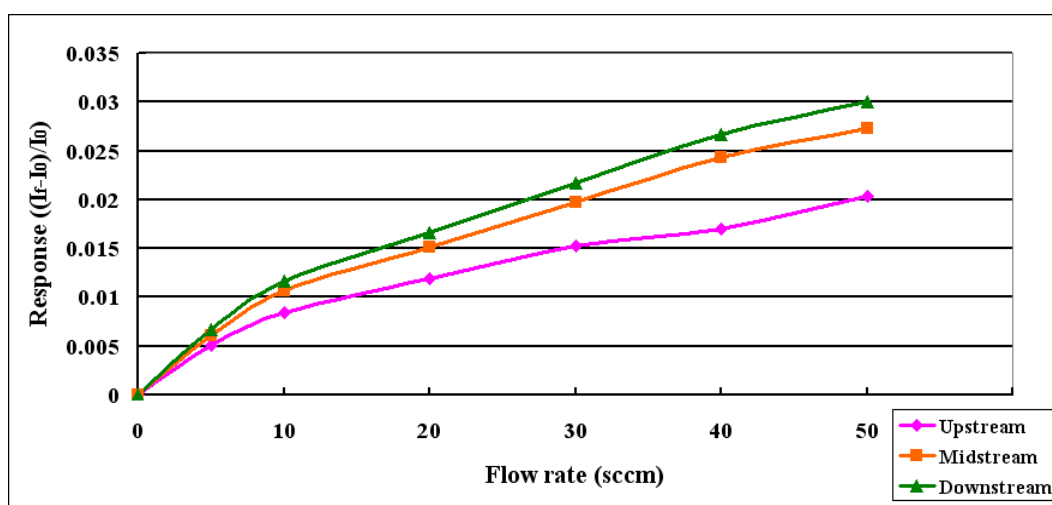


Figure 10. Calibration curves of micro flow sensor.

4.3. Calibration of Micro pressure Sensors

The operating environment of micro reformer was a pressure and thermal coupling environment, so the thermal effect must be considered into correction. A temperature controlled and stable positive pressure chamber environment was required for correction. The pressure correction data acquisition was implemented by Wayne Kerr Electronics 4230 LCR meter. The corrected pressure range was 0~2kgf/cm², the precision of pressure controller was ±0.5%, and the resolution was 0.01kgf/cm². The correction curve of micro pressure sensor is shown in figure 11.

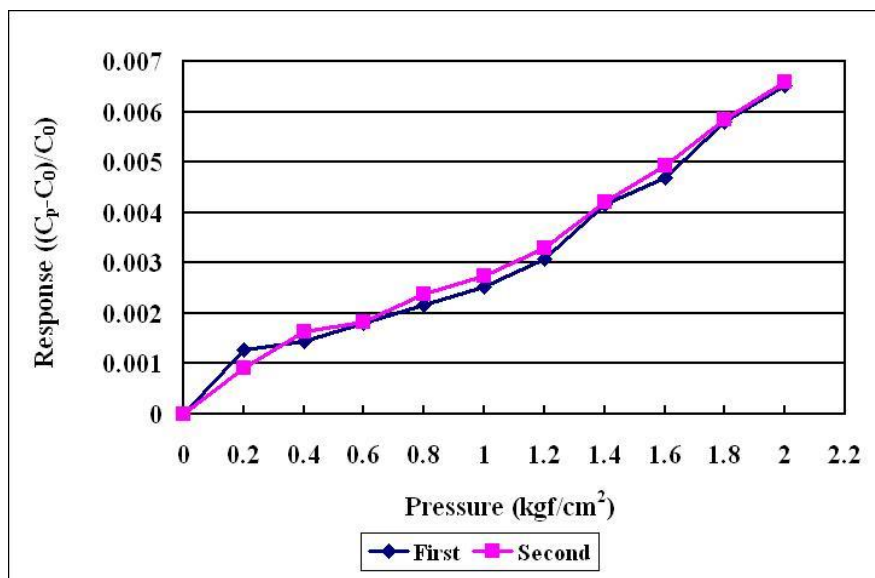


Figure 11. Calibration curves of micro pressure sensor.

4.4. Measurement of the Micro Methanol Reformer

There was only a single micro temperature sensor for the actual temperature distribution in the micro methanol reformer in the past [5]. This study embedded the integrated multifunction micro sensor in the micro reformer, and located it in the upstream, midstream and downstream of flow channel plate. Figure 12 is the schematic diagram of measurement positions of integrated multifunction micro sensor in the micro reformer.

Figure 13 shows the temperature distribution in the upstream, midstream and downstream of flow channel inside the micro reformer during methanol vapor reforming reaction at 270°C. The result showed that the upstream temperature change was larger than midstream and downstream obviously. According to the trends of temperature changes in various blocks, the variation of temperature response decreased by degrees in order of upstream, midstream and downstream. It was because the heat-absorbing reaction of methanol fuel was more severe in the upstream than in midstream and downstream. The mean values of the upstream, midstream and downstream flow channel reaction zones were 262.7°C, 266.4°C and 268.9°C respectively. This was because the extent of heat-absorbing reaction decreased by degrees with the consumption of methanol fuel under the operating conditions.

Figure 14 shows the flow rates in the upstream, midstream and downstream of flow channel in the micro reformer. As seen, the upstream flow rate was 10.8sccm, the midstream was 12.7sccm, and the downstream was 14.4sccm. The difference to the 10sccm infed methanol vapor in the upstream was 0.8sccm, which was due to the reaction between methanol vapor and the catalyst before passing by the micro sensor. The difference between the measured value of downstream flow rate and the estimated value 12.83sccm of post-reaction products (hydrogen, CO, CO₂, unreacted methanol vapor) was 1.57sccm.

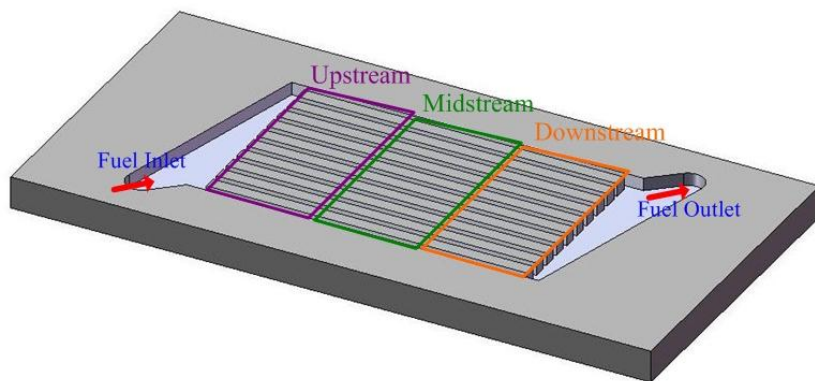
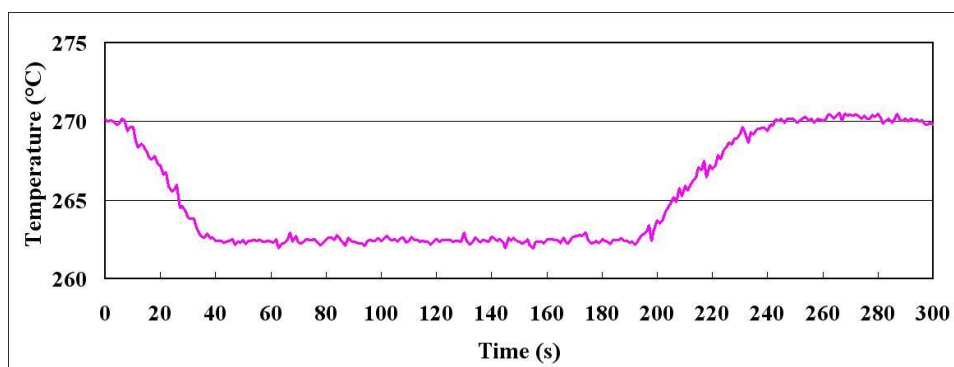
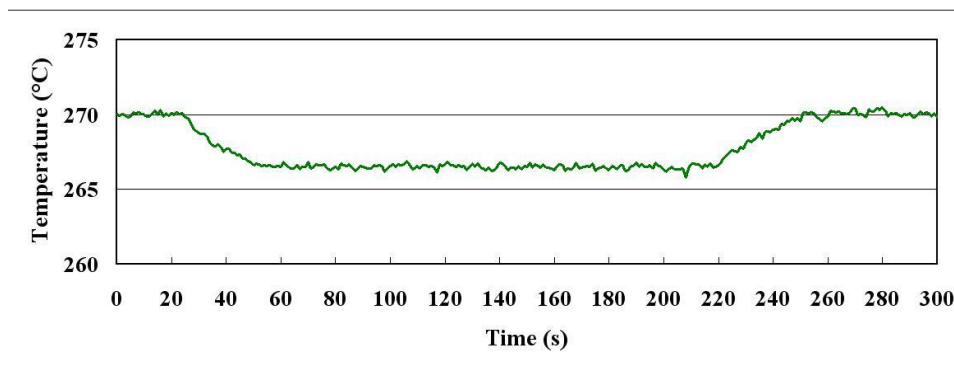


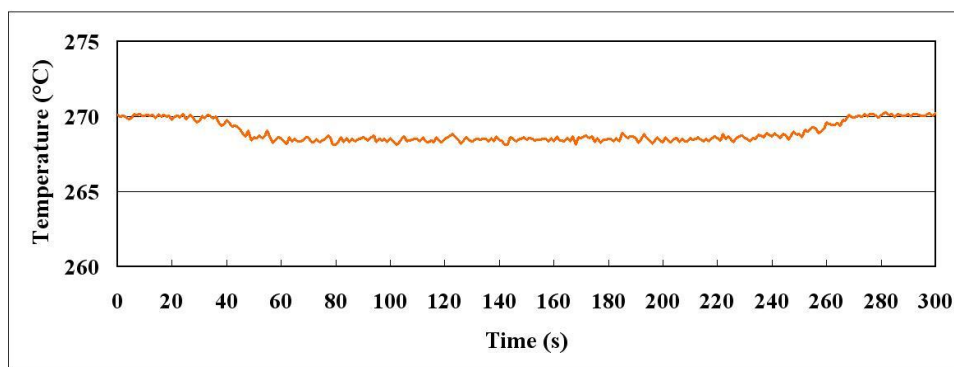
Figure 12. Measurement positions of integrated multifunction micro sensors.



(a) Upstream



(b) Midstream



(c) Downstream

Figure 13. The temperature distribution in the upstream, midstream and downstream of flow channel.

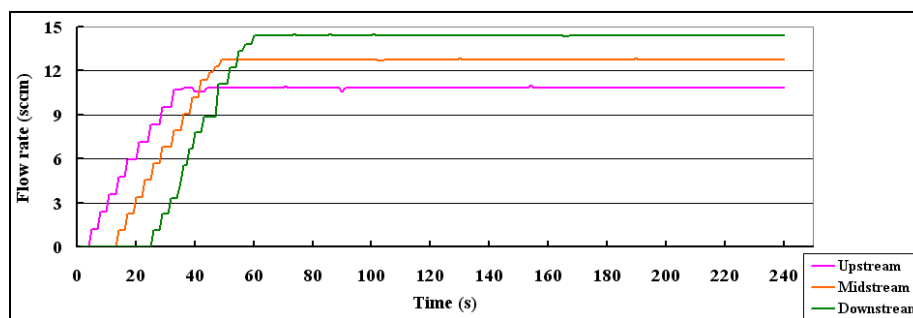


Figure 14. The flow rates in the upstream, midstream and downstream of flow channel.

5. CONCLUSIONS

This study successfully integrated micro temperature, flow and pressure sensors into PI film substrate by using micro-electro-mechanical systems technology to form an integrated multifunction micro sensor. It was used to measure local temperature, flow and pressure distributions in the internal flow channel of micro reformer. It could also measure and record the internal information of micro reformer during reaction instantly. This technology could be used in the studies of improving micro reformer structure design and optimum operating parameters in the future, this contributing to the methanol conversion rate. The findings of this study could be applied to real-time monitoring and adjustment of micro reformer control to obtain the optimum conversion efficiency.

ACKNOWLEDGEMENTS

This work was accomplished with much needed support and the authors would like to thank the financial support of this research from National Science Council of R.O.C. through the grant NSC 100-2221-E-155-034-MY2 and NSC 102-2622-E-155-003. The authors also like to thank Professors Shuo-Jen Lee, Chuin-Tih Yeh, Ho-Shing Wu, Kuen-Song Lin, Yu-Chuan Lin of Yuan Ze University for their valuable advice and assistance in the experiments. In addition, we would like to thank the YZU NENS Common Lab, TKU MEMS Lab for providing access to their research facilities.

References

1. L. Pan, C. Ni, X. Zhang, Z. Yuan, C. Zhang, S. Wang; *Int. J. Hydrogen Energ.* 36 (2011) 1-7.
2. R. Chein, Y. C. Chen, J. Y. Chen, J. N. Chung; *Int. J. Hydrogen Energ.* 37 (2012) 6562-6571.
3. F. P. D'Aleo, H. M. Prasser; *Flow Meas. Instrum.* 24 (2012) 29-35.
4. M. Shikida, K. Yoshikawa, S. Iwai, K. Sato; *Sensor Actuat. A-Phys.* 188 (2012) 2-8.
5. C. Y. Lee, S. J. Lee, C. C. Shen, C. T. Yeh, C. C. Chang, Y. M. Chang; *Int. J. Hydrogen Energ.* 36 (2010) 2869-2876.
6. C. Y. Lee, S. J. Lee, C. C. Shen, C. T. Yeh, C. C. Chang, Y. M. Lo; *Sensors* 11 (2011) 2246-2256.
7. C. Y. Lee, A. Su, Y. C. Liu, P. C. Chan, C. H. Lin; *Sensors* 10 (2010) 3363-3372.
8. C.Y. Lee, P. C. Chan, S.J. Lee; *Sensors* 10 (2010) 11605-11617.
9. C. Y. Lee, S. J. Lee, Y. T. Cheng, Y. M. Chang; *Appl. Mech. Mater.* 284-287 (2013) 1872-1876.